TIDAL EFFECTS ON MFP VIA THE INTIMATE96 TEST

A. TOLSTOY

ATolstoy Sciences, 8610 Battailles Ct., Annandale, VA 22003, USA
E-mail: atolstoy@ieee.org

S. JESUS AND O. RODRÍGUEZ

SiPLAB-FCT, University of Algarve, Faro, Portugal
E-mail: {sjesus,orodrig}@ualg.pt

Examining Intimate96 field data we see clearly the effects of tidal changes, i.e., of changing water depths for a bottom-tethered vertical array at mid-frequencies (300 to 800 Hz). This work will examine the sensitivity of such data via Matched Field Processing (MFP) to tidal changes where the depth varies ± 1.0 m from the nominal of 135 m. Is it possible to invert such data to estimate water depth as a function of time (tides)? Are the data dominated by source range estimates where water depths are known to shift in a predictable fashion as a function of source range errors? Results reported here will be for simulated data.

1 Introduction

Matched Field Processing [1] (MFP) is known to be sensitive to numerous environmental parameters as well as to source location, as seen clearly in the combination test cases SSPMIS, GENLMIS, and SLOPE of the MFP benchmarking workshop of 1993 [2]. Of particular importance are: water depth D (to which many inversion methods are quite sensitive [2, 3]) and source range r_{sou} (a dominant parameter of intense interest [4, 2, 3]). Not only are the accuracies of these two parameters D and r_{sou} critical to MFP performance and to all MFP based inversion techniques, but they are known to be linearly related [5, 6]. That is, they are strongly interrelated.

2 Intimate96 test

In 1996 a shallow water test (approximately 135 m of water) was conducted off the coast of Portugal which included a data set for a fixed source location (range of approximately 5.5 km, depth 92 m) and a fixed vertical, bottom-tethered array (3 working phones) monitored over a 24 hour period. The test configuration for this set is indicated in Fig. 1 with more details in [7–10]. The time window was sufficient to demonstrate obvious tidal effects on a broadband of mid frequency data (300 to 800 Hz) while effectively holding all parameters fixed, e.g., r_{sou}, *except* for water depth D. These data (for one phone) are seen in Fig. 2 (see [10]) where the 24 hours of data have been aligned to begin simultaneously (at 0.3 s). We can clearly see the tidal effects, particularly on the later arriving multipaths, e.g., after 0.5 s, where oscillations are evident. After some basic
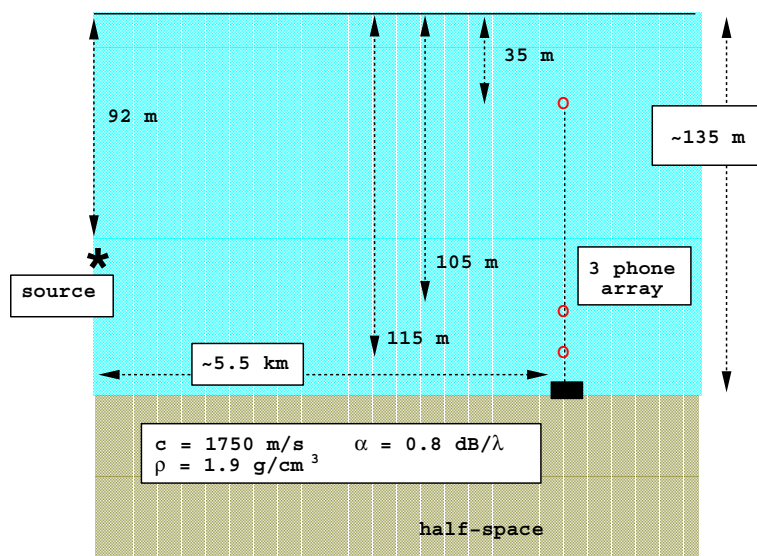
Figure 1. Intimate96 test configuration. Indicated is a source at 92 m depth, in approximately 135 m of water, approximately 5.50 km range from a bottom tethered array of 3 phones at 35, 105, and 115 m depth. The bottom is assumed to be a simple half-space. The sound-speed profile (not shown) is constant with range and refracts energy into the bottom.

MFP processing to produce ambiguity surfaces AMSs) the data (Fig. 3) show similar range fluctuations over 24 hours – if we assume that D is constant while $\hat{r}_{sou}$ varies (Fig. 3, see [10]).

3   Simulated data results

In an effort to examine tidal effects we have simulated the test environment with simple bottom parameters as indicated in Fig. 1, i.e., the bottom is represented as a half-space with parameter values as indicated, and with a downward refracting ocean sound-speed profile. The "data" are generated at a designated frequency by means of RAMGEO, a wide-angle energy-conserving Padé PE propagation model [11, 12]. Increasing attenuation at very deep depths acts as a "false" bottom to prevent the return of bottom penetrating energy, and these "data" have been successfully compared for final confidence to those generated by KRAKEN [12, 13]. The test fields have also been generated by RAMGEO.

3.1   Single Frequency Streaks

An important question becomes: can we resolve, i.e., successfully estimate *simultaneously*, r_{sou} and D? To address this issue, we first examined the source at 320 Hz which assumed data for a true $r_{sou} = 5.50$ km, true $D = 135.0$ m but which allowed the test data to vary in range $5.45 \leq \hat{r}_{sou} \leq 5.85$ km, and in water depth $130.0 \leq \hat{D} \leq 136.0$ m. The high resolution Capon (Minimum Variance: MV) processor [1] results are shown in Fig. 4 where the maximum power 1.10 (for diagonal noise loading 0.1) does appear
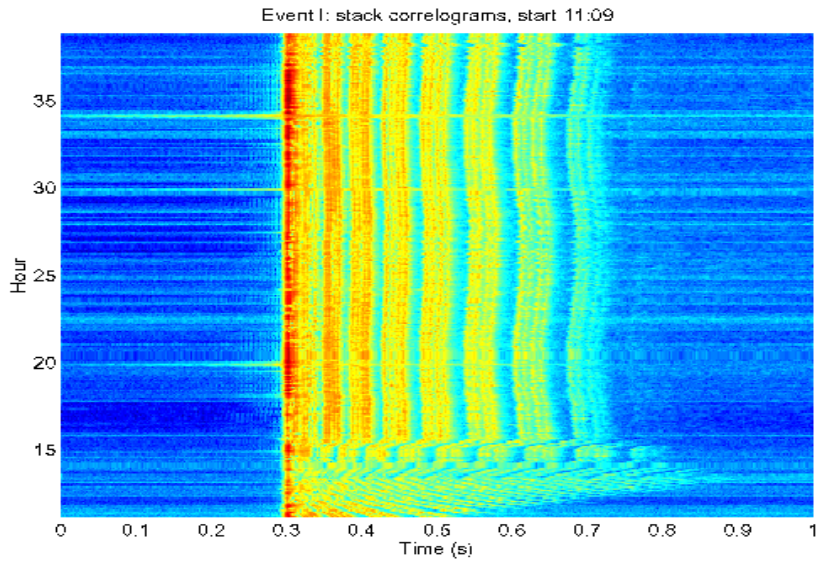
Figure 2. Intimate96 data showing tidal fluctuations for a fixed array and fixed source while time, i.e., water depth, varies over a 24 hour period (courtesy of M.B. Porter).
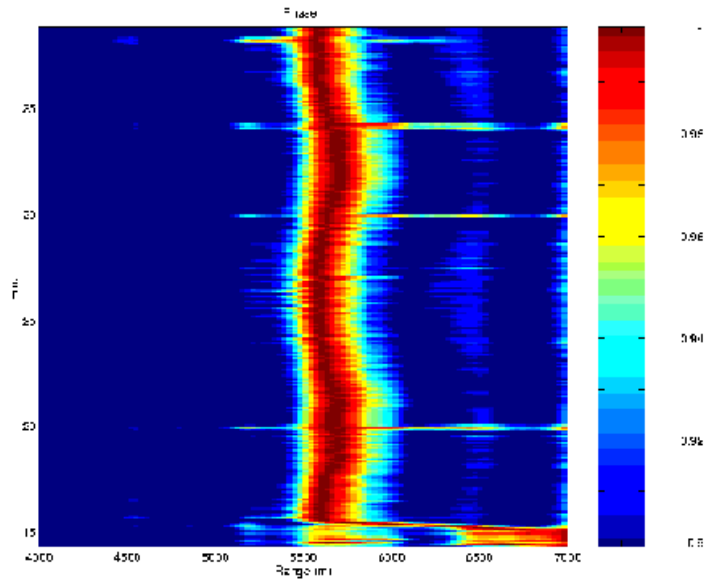

Figure 3. Intimate96 data showing range fluctuations in the AMSs for the data as they vary over a 24 hour period assuming a constant water depth D (courtesy of M.B. Porter).
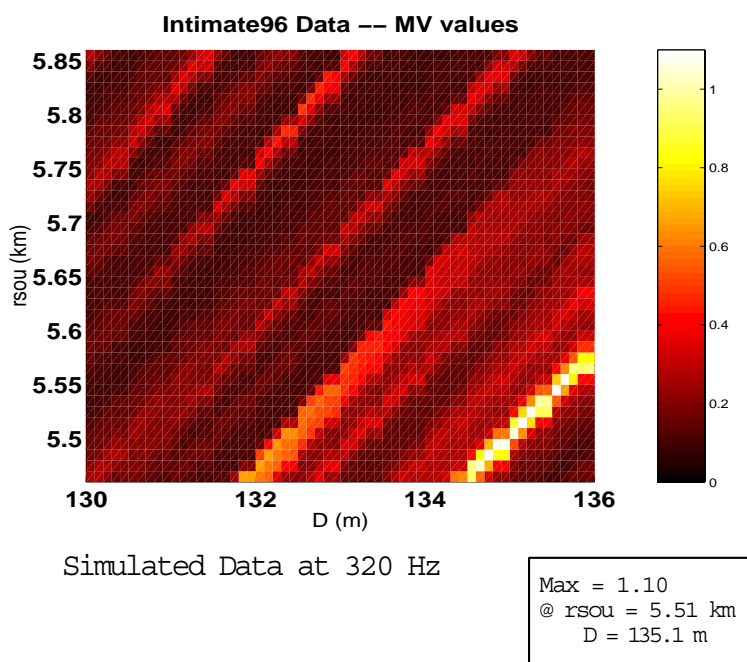
Figure 4. AMS for MV processor for simulated data at 320 Hz. The true source range $r_{sou} = 5.50$ km, true water depth $D = 135$ m. We note the linear relationships between range and water depth.

at the correct range and water depth, as expected. However, we note that there are other estimated ranges and water depths for which the MV power is also quite high, i.e., near 1.10. In particular, these ranges and depths appear along a line passing through the true values. Without knowing either the true source range or the true water depth at a given time, it is impossible to select the true pair of unknown values. We note also that there are other "streaks" in this MV plot, i.e., other $(\hat{r}_{sou}, \hat{D})$ linear combinations with similar slopes, indicating that the usual sidelobes (other phantom solutions) also show similar linear relationships between range and water depth. We see that in general as $\hat{D}$ increases so will $\hat{r}_{sou}$. Moreover, we note that if $\hat{D}$ changes by $+0.1$ m (a very small depth change), then $\hat{r}_{sou}$ will change by $+10.0$ m, a factor of 100.

3.2 Multiple Frequency Streaks

Next, we consider another frequency: 360 Hz. This frequency is also fairly low, but we again see (Fig. 5) the same linear relationship that we saw earlier (Fig. 4) between $\hat{r}_{sou}$ and $\hat{D}$ through the true source range and water depth (5.50 km range, 135 m depth). However, the "sidelobes", i.e., the other streaks, are now at *different* locations. Thus, a broadband BB (multi-frequency) sum of these AMSs will help to suppress these other false solutions. Unfortunately, a BB sum will not help us to select the true range-depth pair along the line through the true solution. That is, we are still unable to simultaneously determine r_{sou} and D.
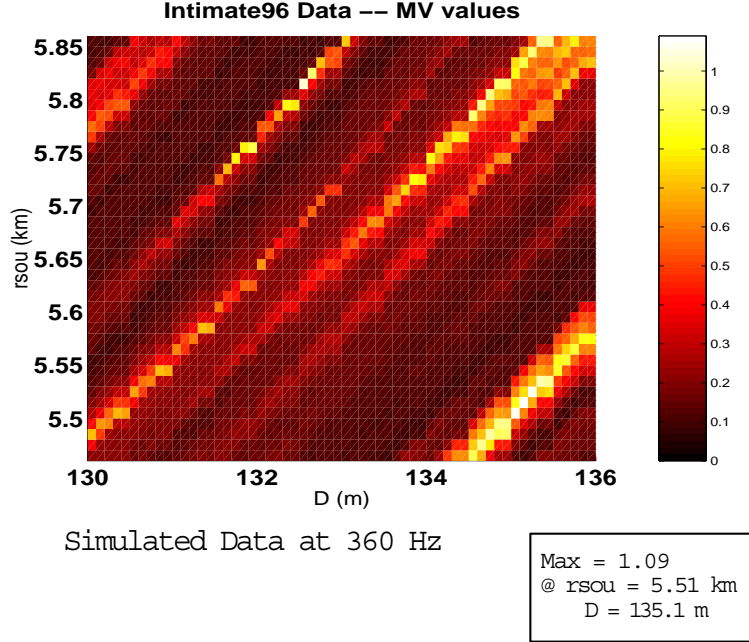
Figure 5. AMS for MV processor for simulated data at 360 Hz. The true source range $r_{sou} = 5.50$ km, true water depth $D = 135$ m. We note the linear relationships between range and water depth. We note also that the sidelobes, i.e., streaks not intersecting the true source range and water depth, are *different* from those at 320 Hz.

3.3   Changing Water Depths

Finally, let us examine the effect of changing water depth on the AMSs. In Fig. 6 we see abbreviated AMSs ($5.46 \leq \hat{r}_{sou} \leq 5.56$ km, $130 \leq \hat{D} \leq 136$ m) at 320 Hz for a variety of "true" water depths mimicking tidal effects. In particular, in the top panel of Fig. 6 the true water depth is 135 m (see Fig. 4) while at next panel the true water depth is now 134.9 m. We note that the sidelobes (streaks) have changed similarly to those which occur at another frequency. However, we still have the same difficulty finding the true source and water depth simultaneously. That is, the true source range and water depth still lie on the same line as before but shifted according to depth (or equivalently, range). Thus, the linear relationship between source range and water depth has not changed. We still can *not* resolve the source range versus water depth ambiguity.

4   Conclusions

We conclude from simulations that:

- there is a linear relationship seen in MFP AMSs between water depth $\hat{D}$ and source range $\hat{r}_{sou}$ (consistent with earlier findings by DelBalzo *et al.*);
- an increase in $\hat{D}$ results in a predictable increase in $\hat{r}_{sou}$ as estimated by MFP (factor of 100);
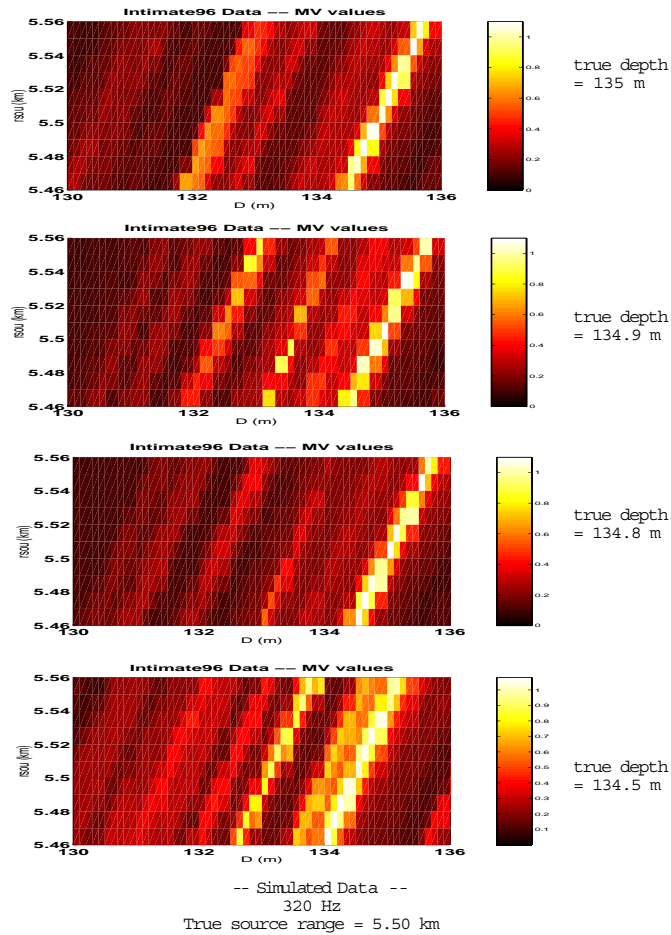
Figure 6. AMSs for MV processor for simulated data at 320 Hz for a source at 5.50 km range and for a variety of true water depths (as indicated).

- multiple frequencies summed incoherently can reduce sidelobe "streaks" in $(\hat{D}, \hat{r}_{sou})$ AMSs but cannot resolve the true (D, r_{sou}), i.e., beyond the basic linear relationship intrinsic to the waveguide;
- multiple time samples allowing for changing D show changing sidelobe "streaks" similar to the behavior seen in multiple frequencies;
- multiple time samples allowing for changing D show translation shifts in the basic linear relationship but still cannot resolve (D, r_{sou}), i.e., the *slope* of the line does not change.

Acknowledgements

References

1. Tolstoy, A., *Matched Field Processing in Underwater Acoustics* (World Scientific Publishing, Singapore, 1993).
2. Porter, M.B. and Tolstoy, A., The matched field processing benchmark problems, *J. Comp. Acoust.* **2**(3), 161–185 (1994).
3. Tolstoy, A., Chapman, N.R. and Brooke, G., Workshop97: Benchmarking for geoacoustic inversion in shallow water, *J. Comp. Acoust.* **(6)**(1&2), 1–28 (1998).
4. Baggeroer, A.B., Kuperman, W.A. and Schmidt, H., Matched field processing: Source localization in correlated noise as an optimum parameter estimation problem, *J. Acoust. Soc. Am.* **83**, 571–587 (1988).
5. DelBalzo, D.R., Feuillade, C. and Rowe, M.M., Effects of water-depth mismatch on matched-field localization in shallow water, *J. Acoust. Soc. Am.* **83**, 2180–2185 (1988).
6. Weinberg, N.L., Clark, J.G. and Flanagan, R.P., Internal tidal influence on deep-ocean acoustic ray propagation, *J. Acoust. Soc. Am.* **56**(2), 447–458 (1974).
7. Jesus, S.M., Porter, M.B., Stephan, Y., Demoulin, X., Rodrigues, O.C. and Coelho, E., Single hydrophone source localization, *IEEE J. Oceanic Eng.* **25**(3), 337–346 (2000).
8. Porter, M.B., Jesus, S.M., Stephan, Y., Coelho, E., Demoulin, X., Single-hydrophone source tracking in a variable environment. In *Proc. 4th European Conference on Underwater Acoustics*, Rome, Italy (1998) pp. 575–580.
9. Porter, M.B., Jesus, S., Stephan, Y., Demoulin, X. and Coelho, E., Exploiting reliable features of the ocean channel response. In *Shallow Water Acoustics,* edited by by R. Zhang and J. Zhou (China Ocean Press, Beijing, 1997).
10. Porter, M.B, Stephan, Y., Demoulin, X., Jesus, S.M. and Coelho, E., Shallow-water tracking in the Sea of Nazare. In *Proc. Undersea Technology'98,* (IEEE Ocean Engineering Society, Tokyo, Japan, 1998).
11. Collins, M.D., A split-step Padé solution for the parabolic equation method, *J. Acoust. Soc. Am.* **93**, 1736–1742 (1993).
12. Jensen, F.B., Kuperman, W.A., Porter, M.B. and Schmidt, H., *Computational Ocean Acoustics* (Amer. Inst. Physics, New York, 1994).
13. Porter, M.B., The KRAKEN normal mode program. Report SM-245, SACLANT Undersea Research Centre, La Spezia, Italy (1991).